Photodissociation Dynamics of ClO Radicals at 248 nm

H. Floyd Davis* and Yuan T. Lee

Chemical Sciences Division, Lawrence Berkeley Laboratory and Department of Chemistry, University of California, Berkeley, California 94720

Received: April 5, 1995; In Final Form: September 21, 1995[⊗]

The photodissociation of ClO radicals produced photolytically in a molecular beam was studied at 248 nm using photofragment translational energy spectroscopy. Excitation into the ClO absorption continuum to the blue of the structured region of the ClO($A^2\Pi \leftarrow X^2\Pi$) spectrum led to dominant (∼97%) formation of $Cl(^2P_{3/2})$ + $O(^1D_2)$ with negligible (<0.5%) production of $Cl(^2P_{1/2})$ + $O(^1D_2)$. The photofragment anisotropy parameter (β) was measured to be 1.2 ± 0.2 for the dominant $Cl(^2P_{3/2})$ + $O(^1D_2)$ channel, significantly less than the limiting value of 2.0 expected for the parallel ClO ($A^2\Pi \leftarrow X^2\Pi$) transition. This indicates that, in the ClO continuum region near 248 nm, absorption to an as yet uncharacterized electronic state [probably $B(^2\Sigma^+)$] carries ∼30% of the oscillator strength. This state, like $ClO(A^2\Pi)$, dissociates primarily to $Cl(^2P_{3/2})$ + $O(^1D_2)$. A second minor photodissociation channel, accounting for approximately 3% of the ClO absorption cross section, leads to production of $Cl(^2P_{1/2})$ + $O(^3P_J)$. As in the photodissociation of ClO below the $A^2\Pi$ convergence limit, this minor channel probably involves predissociation of $ClO(A^2\Pi)$ by one or more as yet uncharacterized repulsive electronic surfaces.

1. Introduction

The ClO radical is an important atmospheric species, playing a key role in catalytic cycles leading to Antarctic ozone depletion.[1−5] At wavelengths shorter than 310 nm, the strong $ClO(A^2\Pi \leftarrow X^2\Pi)$ ultraviolet absorption spectrum shows a series of vibrational bands[6−14] which merge into a broad continuum at wavelengths shorter than 265 nm (Figure 1). The ClO absorption spectrum was first recorded at relatively high resolution by Durie and Ramsay[6] and subsequently reinvestigated by a number of other groups.[7−14] All of the vibrational bands of the $A^2\Pi$ excited state are relatively broad, with the line widths varying from 0.5 to 5.5 cm^{-1}, indicating that even under the structured region of the spectrum predissociation occurs on the picosecond time scale.[6,7,13,14] Consequently, attempts to observe near-ultraviolet fluorescence from $ClO(A^2\Pi)$ have been unsuccessful,[12] and direct near-UV absorption[6−13] or VUV fluorescence[15] from the higher Rydberg levels has been employed for its detection.[15]

Analysis of the $ClO(A^2\Pi)$ convergence limit near 265 nm (Figure 1) led to a ground state dissociation energy of $D_0(ClO)$ = 63.427 ± 0.008 kcal/mol.[9] In the continuum region of the absorption spectrum above the convergence limit, four photodissociation channels are thermodynamically accessible:[9,16]

$$ClO(X^2\Pi) + h\nu \rightarrow Cl(^2P_{3/2}) + O(^3P_J) \quad \Delta H = 63.43 \text{ kcal/mol} \quad (1)$$

$$\rightarrow Cl(^2P_{1/2}) + O(^3P_J) \quad \Delta H = 65.95 \text{ kcal/mol} \quad (2)$$

$$\rightarrow Cl(^2P_{3/2}) + O(^1D_2) \quad \Delta H = 108.78 \text{ kcal/mol} \quad (3)$$

$$\rightarrow Cl(^2P_{1/2}) + O(^1D_2) \quad \Delta H = 111.30 \text{ kcal/mol} \quad (4)$$

The thermodynamic quantities for channels 1 and 2 refer to formation of ground state $O(^3P_2)$. Spin−orbit excited levels lie at 123 cm^{-1} ($^3P_1$) and 254 cm^{-1} ($^3P_0$).[16] At 248.5 nm (E = 115.01 kcal/mol), channels 1−4 are accessible. At this wavelength, the ClO absorption cross section[10] is more than 1 order of magnitude greater than that for OClO.[17,18] Near 397 nm, on the other hand, ClO is transparent,[10] but OClO absorbs strongly, dissociating primarily to $ClO(v=0) + O(^3P_J)$.[19,20] From these considerations, photodissociation of OClO near 397 nm should be a clean source of $ClO(v=0)$ for photodissociation and crossed beam reactive scattering studies. Because of the small OClO absorption cross section at 248 nm, a study of ClO photodissociation at this wavelength should not be affected significantly by the unavoidable presence of OClO impurity.

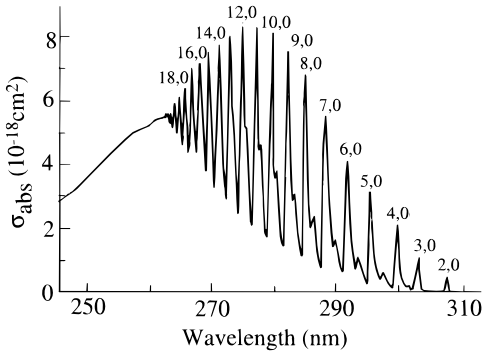

Figure 1. $ClO(A^2\Pi \leftarrow X^2\Pi)$ absorption spectrum (adapted from ref 10a).

The excited $ClO(A^2\Pi)$ potential correlates asymptotically[6] to $Cl(^2P_{3/2})$ + $O(^1D_2)$ (Figure 2). At wavelengths longer than 265 nm, thermodynamics dictates formation of ground state oxygen atoms, $O(^3P_J)$ (channels 1 or 2), from predissociation of the optically prepared $ClO(A^2\Pi)$ states by one or more as yet uncharacterized electronic states correlating to $Cl(^2P_{1/2,3/2})$ + $O(^3P_J)$. Although excitation into the continuum region of the $ClO(A^2\Pi)$ state above the convergence limit is likely to lead to its asymptotic products, *i.e.*, $Cl(^2P_{3/2})$ + $O(^1D_2)$,[6] the involvement of other electronic states (either by direct absorption or by predissociation) can lead to other photodissociation channels.

To our knowledge, there has been no previous experimental determination of the product channels from ClO photodisso-

* To whom correspondence should be addressed at Department of Chemistry, Baker Laboratory, Cornell University, Ithaca, New York 14853-1301.

[⊗] Abstract published in *Advance ACS Abstracts,* December 1, 1995.

0022-3654/96/20100-0030$12.00/0

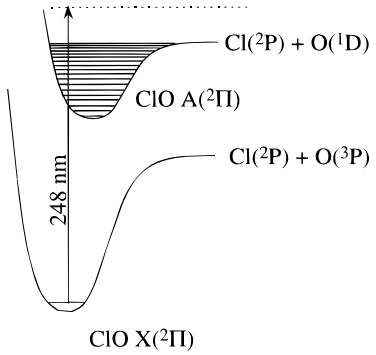

Figure 2. Energy level diagram for ClO photodissociation.

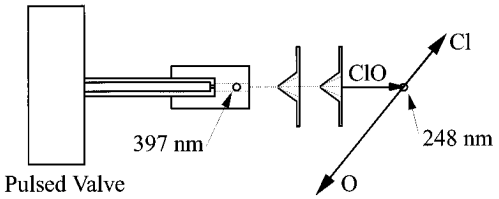

Figure 3. Schematic of the photolytic radical source.

ciation at any wavelength. From the previous spectroscopic studies, it has been possible to infer picosecond dissociation time scales for all ClO($A^2\Pi$) levels in the structured region of the absorption spectrum below the convergence limit.[13] In the higher energy region above the convergence limit, it is not possible to gain insight into carrier(s) of the oscillator strength or dynamics of the ensuing dissociation process using conventional spectroscopic methods, because of the continuous nature of the absorption spectrum. Thus, we have studied the photodissociation dynamics of ClO in the continuum region at 248 nm using photofragment translational energy spectroscopy. On the basis of the large signal levels seen in this experiment, the intensity of our photolytic radical source is expected to be sufficient to permit future crossed molecular beam reactive scattering studies of ClO radicals with small polyatomic molecules.

2. Experimental Section

The experiment was conducted using a molecular beam apparatus equipped with a rotatable molecular beam source and fixed mass spectrometer detector.[19−21] A ClO radical beam was generated by photodissociation of OClO followed by supersonic expansion. The design of the pulsed photolytic radical beam source is similar to that described originally by Smalley and co-workers[22,23] and more recently by Hintsa *et al.*[24] As shown in Figure 3, the source consists of a Teflon photolysis region attached to the nozzle of a piezoelectric pulsed valve.[25] A mixture of 10% OClO/He was prepared *in situ* as described previously.[19,26] For OClO photolysis, output from an excimer pumped dye laser (Laser 1; Lambda-Physik FL2002) was focused to a spot size of approximately 1 mm, as measured at the crossing point of the laser with the molecular beam. The laser was aligned to pass through a 1 mm cylindrical hole drilled perpendicular to the beam axis through the Teflon photolysis region. The wavelength of laser 1 was tuned to the OClO $^2A_2$-(6,0,0) ← $^2B_1$(0,0,0) absorption peak near 397 nm.[17,18] The total stagnation pressure of the room temperature nozzle was 1 atm, and the repetition rate of the pulsed valve and lasers was 50 Hz. After a time delay appropriate for transport of the radicals through two skimmers into the interaction zone approximately 10 cm away, the 248 nm excimer laser (Laser 2; Lambda-Physik EMG 202MSC) was triggered to photodissociate the ClO radicals. The 248 nm laser also triggered the multichannel scaler used for time-of-flight detection of the atomic products.[19−21,27] Time-of-flight spectra were obtained under two sets of conditions. To study the photodissociation of OClO at 248 nm, experiments were conducted with laser 1 blocked and laser 2 on. To study the photodissociation of ClO at 248 nm, data were recorded with both lasers on. Spectra were recorded with the mass spectrometer set at $m/e = 35$ (Cl^+), $m/e = 16$ (O^+), $m/e = 51$ (ClO^+) and $m/e = 67$ (ClO_2^+).

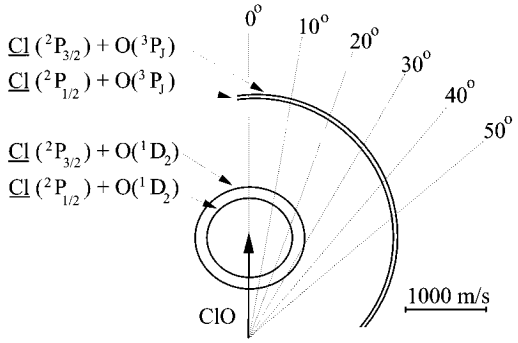

Figure 4. Newton diagram in velocity space for ClO photodissociation at 248 nm. Circles correspond to center of mass velocities of Cl atoms produced in channels 1−4.

In most experiments, the 248 nm laser was unpolarized. To measure the Cl + O photofragment anisotropy from ClO photodissociation, the 248 nm beam was polarized to >98% using a 16 plate "pile of plates" polarizer. The polarized excimer laser beam was apertured to a diameter of 6 mm, directed through a quartz double Fresnel rhomb (Optics for Research) and focused to ~3 mm diameter at the interaction region. The velocity of the OClO beam was measured using a TOF chopper wheel that could be moved into the molecular beam. Photodissociation experiments were conducted with the molecular beam at 20° and 50° from the detector axis. Since this apparatus utilizes a rotatable molecular beam source, two different optical paths were employed for the OClO photodissociation laser (laser 1), facilitating production of the ClO beam at two different nozzle locations. Either of the two laser paths could be conveniently selected using a beam steering mirror mounted on a translational stage. Product TOF spectra and polarization rotation dependence data were analyzed using the program CMLAB2, as described previously.[27,28] The delay times between opening of the pulsed valve and firing the photolysis laser (t_1), and the delay between the two lasers (t_2), were iteratively adjusted to optimize the intensity of the Cl product signal from ClO photodissociation, as measured at a beam detector angle of 20°.

3. Results and Discussion

3.1. Photodissociation of ClO at 248 nm. The Newton diagram for photodissociation of ClO at 248 nm is shown in Figure 4. The time-of-flight (TOF) spectrum for $m/e = 35$ ($^{35}Cl^+$), obtained with both lasers on, is shown in Figure 5. Laser 1 was tuned to the peak of the OClO (6,0,0) band near 397 nm, which we have found in other experiments to dissociate primarily to ClO(v=0) + O(^{3}P).[20] Comparison of the TOF spectra shown in Figure 5 with that from OClO photodissociation (*i.e.*, with laser 1 off) showed a negligible contribution from photodissociation of residual OClO in the beam. The dominant two peaks shown in Figure 5 are very narrow and must correspond to the atomic products from photodissociation of a diatomic molecule. They cannot result from Cl_2 photolysis since (1) Cl_2 has an extremely small absorption cross section[29] at 248 nm and (2) the possible Cl_2 dissociation channels, Cl($^2P_{3/2}$) +

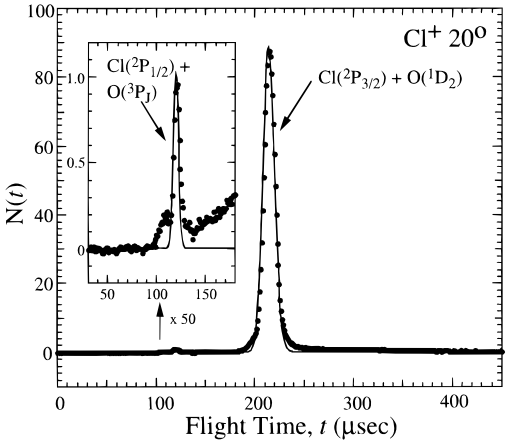

Figure 5. Cl TOF spectrum from photodissociation of ClO at 248 nm. In the inset, the vertical axis for $t = 30-180$ μs is expanded by a factor of 50. The solid lines are calculated TOF assuming 97% yield of $Cl(^2P_{3/2}) + O(^1D_2)$ and 3% $Cl(^2P_{1/2}) + O(^3P_J)$.

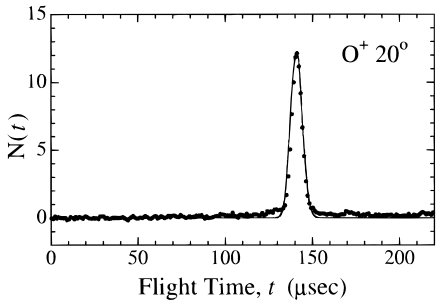

Figure 6. O atom TOF spectrum from ClO photodissociation at 248 nm, recorded at 20°.

TABLE 1: Product Channels from ClO Photodissociation at 248 nm

product channel	contribution, %
$Cl(^2P_J) + O(^3P_J)$	3 ± 1^a
$Cl(^2P_{3/2}) + O(^1D_2)$	97 ± 1
$Cl(^2P_{1/2}) + O(^1D_2)$	<0.5

[a] The TOF spectrum indicates that the $O(^3P_J)$ is primarily accompanied by formation of excited $Cl(^2P_{1/2})$.

$Cl(^2P_{3/2})$ or $Cl(^2P_{1/2}) + Cl(^2P_{3/2})$, are predicted to give different TOF spectra.[16,30,31] Furthermore, the observation of the momentum matched atomic oxygen fragment at $m/e = 16$ (Figure 6) confirms that the dominant peak results from photodissociation of ClO.

The recoil energies imparted to the atomic fragments in channels 1−4 are the differences between the photon energy (115.0 kcal/mol) and the reaction endoergicities. Using the calculated recoil energies, the measured ClO beam velocity distribution, and the known apparatus function, we simulated the Cl TOF spectrum by iteratively adjusting the relative contributions for channels 1−4. The simulated Cl TOF spectrum is shown as a solid line in Figure 5, and the relative contributions of channels 1−4 are summarized in Table 1.

The small fast peak in the Cl TOF spectrum (Figure 5, 120 μs) is located at the time corresponding to formation of $O(^3P_J)$. In the inset, we have expanded the vertical scale of this region by a factor of 50. This fast peak cannot be seen in the O TOF (Figure 6) due to the much larger background count rate at $m/e = 16$ than at $m/e = 35$. In Figure 7, we have shown the calculated TOF spectrum assuming production of $Cl(^2P_{1/2}) + O(^1D_2)$ for the slow peak and $Cl(^2P_{3/2}) + O(^3P_J)$ for the fast peak. Clearly, there is negligible production of $Cl(^2P_{1/2}) + O(^1D_2)$ from photodissociation of ClO at 248 nm. As can be

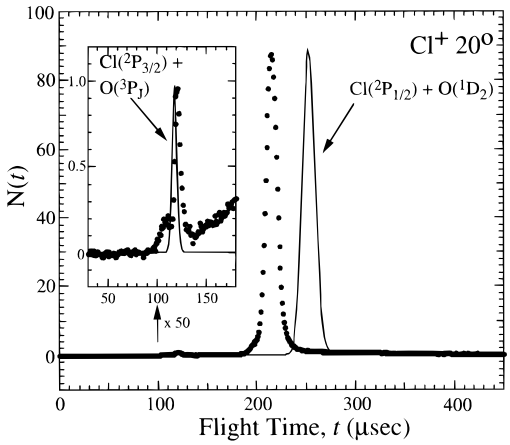

Figure 7. Same as Figure 5, but the solid lines are calculated TOF assuming production of $Cl(^2P_{1/2}) + O(^1D)$ and $Cl(^2P_{3/2}) + O(^3P)$. The fit to the experimental data is poorer than in Figure 5.

seen by comparing the insets in Figures 5 and 7, the calculated contribution assuming $Cl(^2P_{3/2}) + O(^3P_J)$ gives a somewhat poorer fit to the sharp peak than that shown in Figure 5, which assumed production of $Cl(^2P_{1/2}) + O(^3P_J)$. We thus conclude that most of the Cl atoms correlated to $O(^3P_J)$ are spin−orbit excited $Cl(^2P_{1/2})$.

As shown in the inset to Figure 5, a contribution to the Cl TOF at $t = 100-150$ μs is observed which cannot be attributed to 248 nm photodissociation of ClO or ClO_2. This signal was only seen with both lasers on and appears to result from photodissociation of a higher oxide of chlorine. Previous kinetic studies have shown that a number of reactions occur following formation of $ClO + O(^3P)$ in the presence of OClO:[31−34]

$$ClO + OClO + M \rightarrow Cl_2O_3 + M \quad (5)$$

$$ClO + ClO + M \rightarrow (ClO)_2 + M \quad (6)$$

$$OClO + O(^3P) + M \rightarrow ClO_3 + M \quad (7)$$

All of these products absorb significantly at 248 nm[31−34] and are likely to be present in the beam to an unknown extent. Further characterization of these constituents will be required before these minor contributions can be properly understood.

3.2. Polarization Dependence. The ground state and first excited state of ClO are both $^2\Pi_i$.[6] Spectroscopic measurements[9] indicate that the spin−orbit coupling constants for the X and A states are 318 and 520 cm^{-1}, respectively, and both show coupling close to Hund's case (a). The angular distribution for the $Cl(^2P_{3/2}) + O(^1D_2)$ products was measured by rotating the polarization of the 248 nm laser and monitoring the $Cl(^2P_{3/2})$ at 20°. The resulting angular distribution is shown in Figure 8. Since the ClO $A(^2\Pi_{3/2} \leftarrow X^2\Pi_{3/2})$ excitation is a parallel transition ($\Delta\Omega = 0$), we expect a highly anisotropic angular distribution with the atoms preferentially scattered (in the center-of-mass (CM) frame) parallel to the electric vector of the laser.

The normalized CM angular distribution for the atomic products from photodissociation of a diatomic molecule is often[35−37] represented by

$$f(\theta) = (1/4\pi)[1 + \beta P_2(\cos\theta)] \quad (8)$$

where $\beta = 2$ for a parallel ($\Delta\Omega = 0$) transition and $\beta = -1$ for a perpendicular ($\Delta\Omega = \pm 1$) transition. From the fit of eq 8 to the data shown in Figure 8, we find that $\beta = 1.2 \pm 0.2$ for the dominant photodissociation channel forming $Cl(^2P_{3/2}) + O(^1D_2)$.

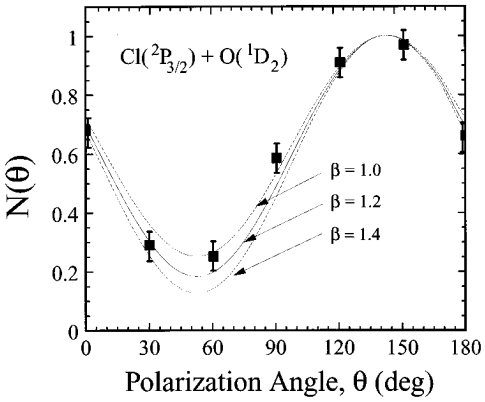

Figure 8. Polarization dependence for $Cl(^2P_{3/2}) + O(^1D_2)$ channel. $\theta = 0$ and 180° corresponds to polarization along the detector axis.

This is significantly less than the limiting value of $\beta = 2$ expected for a pure parallel $A^2\Pi \leftarrow X^2\Pi$ transition. Following absorption at 248 nm, $ClO(A^2\Pi)$ is unbound with respect to dissociation to $Cl(^2P_{3/2}) + O(^1D_2)$, so dissociation is expected to be prompt, without significant rotation of the ClO parent before dissociation. At high laser powers, saturation effects may lead to some reduction of the measured anisotropy parameter.[36,37] In our polarization study, the pulse energy was 1 mJ and the laser spot diameter was 3 mm, corresponding to 1.76×10^{16} photons cm^{-2}. Using a ClO absorption cross section[10] of 2×10^{-18} cm^2, only 3.5% of the molecules are dissociated in the laser pulse so it is unlikely that saturation effects explain why our value of β falls considerably lower than 2.0.

In the derivation of eq 8, it is assumed that the dissociation is rapid on the time scale of parent rotation and that the tangential velocity of the fragments due to parent rotation is negligible compared to the fragment recoil velocity.[35−37] Although the first assumption is reasonable, it is important to note that the relative translational energy imparted to the $Cl(^2P_{3/2}) + O(^1D_2)$ fragments is only 6.2 kcal/mol, leading to a center-of-mass Cl atom recoil velocity (u) of 680 m/s. According to Wilson and co-workers,[37] the effect of parent rotation is to diminish the photofragment anisotropy by a factor of $P_2(\alpha) = {}^1/_2(3\cos^2\alpha - 1)$, where

$$\alpha = \sin^{-1}\left(\frac{\pi k T m_2}{2m_1(m_1 + m_2)u^2}\right)^{1/2} \qquad (9)$$

In eq 9, α is the angle between the tangential component of the parent rotational velocity, v_t, and the fragment recoil velocity, u. The masses of the measured fragment and the counterfragment are denoted by m_1 and m_2, respectively, and T is the beam temperature. Substituting the appropriate values into eq 9, if 100 K is used as an absolute upper limit to the rotational temperature (it probably lies near 15 K), the maximum decrease in the anisotropy parameter is by a factor of 0.93, *i.e.*, from 2.0 to 1.86. Since we measured a value of 1.2 ± 0.2, the contribution from tangential rotational motion in the parent molecule cannot explain our result.

The most reasonable explanation for our observation that $\beta = 1.2$ is that at least one other ClO electronic state involving a perpendicular $\Delta\Omega = \pm 1$ transition carries some oscillator strength at 248 nm. Using an anisotropy parameter of 1.2, this would be consistent with ~70% of the absorption cross section leading to the $A(^2\Pi)$ state, with the remaining ~30% undergoing a perpendicular transition ($\Delta\Omega = \pm 1$) to a state of $^2\Sigma$ or $^2\Delta$ symmetry. To date, the only experimentally observed states of ClO lying above the $A(^2\Pi)$ state are the C, D, E, and F levels above 58 000 cm^{-1}.[39,40] These states are best described as Rydberg levels. However, a number of other relatively low-lying electronic states of ClO above $A(^2\Pi)$ should be accessible by absorption of a single UV photon. From the observed Λ-type doubling seen in the microwave spectrum of $ClO(A^2\Pi)$, Amano *et al.*[41] estimated that the $ClO(B^2\Sigma^+)$ state probably lies near 31 000 cm^{-1}. Subsequent work by Coxon *et al.*[9] also provided evidence for the existence of a $^2\Sigma^+$ state, but at slightly higher estimated energy (35 200 cm^{-1}). Barton and co-workers[8] compared the high-resolution ClO absorption spectrum to calculated $A(^2\Pi) \leftarrow X^2(\Pi)$ absorption cross sections. They concluded that a continuous absorption to at least one other electronic state of ClO exists under the higher v' bands in the structured region of the ClO absorption near 270 nm but did not attempt to provide a quantitative measure of its contribution.

All of these previous, indirect observations point to the existence of a $^2\Sigma^+$ state at 31 000−35 000 cm^{-1}.[8,9] In the structured region of the ClO absorption spectrum, it is known that the absorption line widths are actually the *narrowest* near 265 nm, just below the A state continuum.[13] However, as shown in Figure 1, the region between these peaks does not fall to the base line. This suggests that a broad continuum absorption may be present even under the structured region of the $A(^2\Pi) \leftarrow X(^2\Pi)$ spectrum. Our photofragment anisotropy measurement indicates that the state carrying this oscillator strength at 248 nm is accessed by a perpendicular transition, indicating that it must be of $^2\Sigma$ or $^2\Delta$ symmetry. The previous identification of a $^2\Sigma^+$ state in this wavelength region is thus consistent with our photodissociation results. Furthermore, we conclude that this state, when accessed at 248 nm, promptly dissociates to $Cl(^2P_{3/2}) + O(^1D_2)$. It is important to note that the state accessed in our experiment by a perpendicular transition at 248 nm cannot be the state responsible for predissociation of $ClO(A^2\Pi)$ at $\lambda > 260$ nm, since the products in that wavelength range must be $Cl(^2P_J) + O(^3P_J)$.

An interesting question regards the mechanism for the 3% formation of ground state $Cl(^2P_J) + O(^3P_J)$ fragments. Due to the very small signal level for this channel, we were not able to undertake a polarization dependence study using low laser powers to avoid saturation effects. However, in view of the strong predissociation of the $^2\Pi$ state to these products at longer wavelengths, it is likely that the minor $Cl(^2P_J) + O(^3P_J)$ channel seen in our experiment involves a similar mechanism. However, it is important to note that an analysis of the line widths of the $A^2\Pi$ state of ClO has suggested that more than one interacting repulsive state is likely to be involved.[14] Clearly, electronic structure calculations on the ClO radical would provide useful insight into the dynamics of absorption and photodissociation processes above and below the $^2\Pi$ convergence limit.

4. Conclusions

We have generated an intense, internally cold ClO radical beam by photodissociation of OClO near 400 nm followed by pulsed supersonic expansion. Using photofragment translational energy spectroscopy, we have determined the branching ratios for the photochemical decay channels of ClO at 248 nm. We find that the dominant channel (97%) is production of $Cl(^2P_{3/2}) + O(^1D_2)$, with negligible $Cl(^2P_{1/2}) + O(^1D_2)$, consistent with the theoretical analysis by Durie and Ramsay indicating that $ClO(A^2\Pi)$ correlates asymptotically to $Cl(^2P_{3/2}) + O(^1D_2)$.[6] We also observe a small contribution (~3%) from $O(^3P_J)$ production. Our data indicate that the Cl atom recoil partner in this minor channel is primarily spin−orbit excited $Cl(^2P_{1/2})$. The measured photofragment anisotropy parameter for the dominant $Cl(^2P_{3/2}) + O(^1D_2)$ channel indicates that, in addition to the known $A(^2\Pi)$ state, one or more other electronic states of ClO having $^2\Sigma$ or

$^2\Delta$ symmetry (likely $^2\Sigma^+$) are accessed upon absorption at 248 nm, also dissociating primarily to $Cl(^2P_{3/2}) + O(^1D_2)$.

Acknowledgment. Some of the equipment used in this work was provided by the Office of Naval Research under Contract N00014-89-J-1297. This work was supported by the Director, Office of Energy Research, Office of Basic Energy Sciences, Chemical Sciences Division of the U.S. Department of Energy, under Contract DE-AC03-76F00098.

References and Notes

(1) Anderson, J. G.; Toohey, D. W.; Brune, W. H. *Science* **1991**, *251*, 39.
(2) Farman, J. C.; Gardiner, B. G.; Shankin, J. D. *Nature* **1985**, *315*, 207.
(3) Molina, L. T.; Molina, M. J. *J. Phys. Chem.* **1987**, *91*, 433.
(4) Salawitch, R. J.; *et al. Science* **1993**, *261*, 1146.
(5) Hamill, P.; Toon, O. B. *Phys. Today* **1991**, *44*, 34 and references therein.
(6) Durie, R. A.; Ramsay, D. A. *Can. J. Phys*. **1958**, *36*, 35.
(7) Coxon, J. A.; Jones, W. E.; Skolnik, E. G. *Can. J. Phys*. **1976**, *54*, 1043.
(8) Barton, S. A.; Coxon, J. A.; Roychowdhury, U. K. *Can. J. Phys*. **1984**, *62*, 473.
(9) Coxon J. A.; Ramsay, D. A. *Can. J. Phys.* **1976,** *54*, 1034.
(10) (a) Mandelman, M.; Nicholls, R. W. *J. Quant. Spectrosc. Radiat. Transfer* **1977**, *17*, 483. (b) Simon, F. G.; Schneider, W. M.; Moortgat, G. K.; Burrows, J. P. *J. Photochem. Photobiol. A: Chem.* **1990**, *55*, 1.
(11) (a) Trolier, M.; Mauldin, R. L.; Ravishankara, A. R. *J. Phys. Chem.* **1990**, *94*, 4896. (b) Wine, P. H.; Ravishankara, A. R.; Philen, D. L.; Davis, D. D.; Watson, R. T. *Chem. Phys. Lett.* **1977**, *50*, 101.
(12) Clyne, M. A. A.; McDermid, I. S.; Curran, A. H. *J. Photochem*. **1976**, *5*, 201.
(13) McLoughlin, P. W.; Park, C. R.; Wiesenfeld, J. R. *J. Mol. Spectrosc*. **1993**, *162*, 307.
(14) Bunker, P. R.; Klein, P. C. *Chem. Phys. Lett.* **1981**, *78*, 552.
(15) Matsumi, Y.; Shamsuddin, S. M.; Kawasaki, M. *J. Chem. Phys*. **1994**, *101*, 8262.
(16) Chase, M. W., Jr.; Davies, C. A. ; Downey, J. R.; Frurip, D. J. ; McDonald, R. A.; Syverud, A. N. *J. Phys. Chem. Ref. Data*. **1981**, *14*, Suppl. 1 (*JANAF Thermochemical Tables*, 3rd ed.)
(17) Wahner, A.; Tyndall, G. S.; Ravishankara, A. R. *J. Phys. Chem*. **1987**, *91*, 2734.
(18) (a) Richard, E. C.; Vaida, V. *J. Chem. Phys*. **1990**, *94*, 153. (b) *J. Chem. Phys.* **1990**, *94*, 163.
(19) Davis, H. F.; Lee, Y. T. *J. Phys. Chem*. **1992**, *96*, 5681.
(20) Davis, H. F.; Lee, Y. T. *J. Chem. Phys*., to be published.
(21) Wodtke, A. M.; Lee, Y. T. *J. Phys. Chem*. **1985**, *89*, 4744.
(22) Monts, D. L.; Dietz, T. G.; Duncan, M. A., Smalley, R. E. *Chem. Phys*. **1980**, *45*, 133.
(23) Powers, D. E.; Hopkins, J. B.; Smalley, R. E. *J. Phys. Chem*. **1981**, *85*, 2711.
(24) Hintsa, E. J.; Zhao, X.; Jackson, W. M.; Miller, W. B.; Wodtke, A. M; Lee, Y. T. *J. Phys. Chem*. **1991**, *95*, 2799.
(25) Proch, D.; Trickl, T. *Rev. Sci. Instrum*. **1989**, *60*, 713.
(26) Derby, R. I.; Hutchinson,W. S. *Inorg. Synth*. **1953**, *4*, 152.
(27) Minton, T. K.; Nathanson, G. M.; Lee, Y. T. *J. Chem. Phys*. **1987**, *86* 1991.
(28) Zhao, X. Ph.D. Thesis, University of California, Berkeley, 1988 (LBL-26332).
(29) Okabe, H. *Photochemistry of Small Molecules*, J. Wiley and Sons: New York, 1978.
(30) Busch, G. E.; Mahoney, R. T.; Morse, R. I.; Wilson, K. R. *J. Chem. Phys*. **1969**, *51*, 449.
(31) Colussi, A. J.; Sander, S. P.; Friedl, R. R. *J. Phys. Chem*. **1992**, *96*, 4442.
(32) Demore, W. B.; Tschuikow-Roux, E. *J. Phys. Chem*. **1990**, *94*, 5856.
(33) Gleason, J. F.; Nesbitt, F. L.; Stief, L. J. *J. Phys. Chem*. **1994**, *98*, 126
(34) (a) Burkholder, J. B.; Mauldin, R. L.; Yokelson, R. J.; Solomon, S.; Ravishankara, A. R. *J. Phys. Chem*. **1993**, *97*, 7597. (b) Burkholder, J. B.; Orlando, J. J.; Howard, C. J. *J. Phys. Chem.* **1990**, *94*, 687.
(35) Zare, R. *J. Photochem*. **1972**, *4*, 1.
(36) Jonah, C. *J. Chem. Phys*. **1971**, *55*, 1915.
(37) Busch, G. E.; Wilson, K. R. *J. Chem. Phys.* **1972**, *56*, 3638.
(38) Oldman, R. J.; Sander, R. K.; Wilson, K. R. *J. Chem. Phys*. **1975**, *63*, 4252.
(39) Basco, N.; Morse, R. D. *J. Mol. Spectrosc*. **1973**, *45*, 35.
(40) Coxon, J. A. *Can. J. Phys*. **1979**, *57*, 1538.
(41) Amano, T.; Hirota, E.; Morino, Y. *J. Mol. Spectroc*. **1968**, *27*, 257.